Electronic Supporting Information

Alkyl-functionalization of 3,5-*bis*(2-pyridyl)-1,2,4,6-thiatriazine

Elizabeth Kleisath, [a,b] *Nathan J. Yutronkie,* [a,b] *Ilia Korobkov,* [a] *Bulat M. Gabidullin* [a] *and Jaclyn L. Brusso* *[,a,b]

[a] Department of Chemistry and Biomolecular Science and [b] Centre for Catalysis Research and Innovation, University of Ottawa, Ottawa, Ontario K1N 6N5, Canada.

Contents (23 pages)

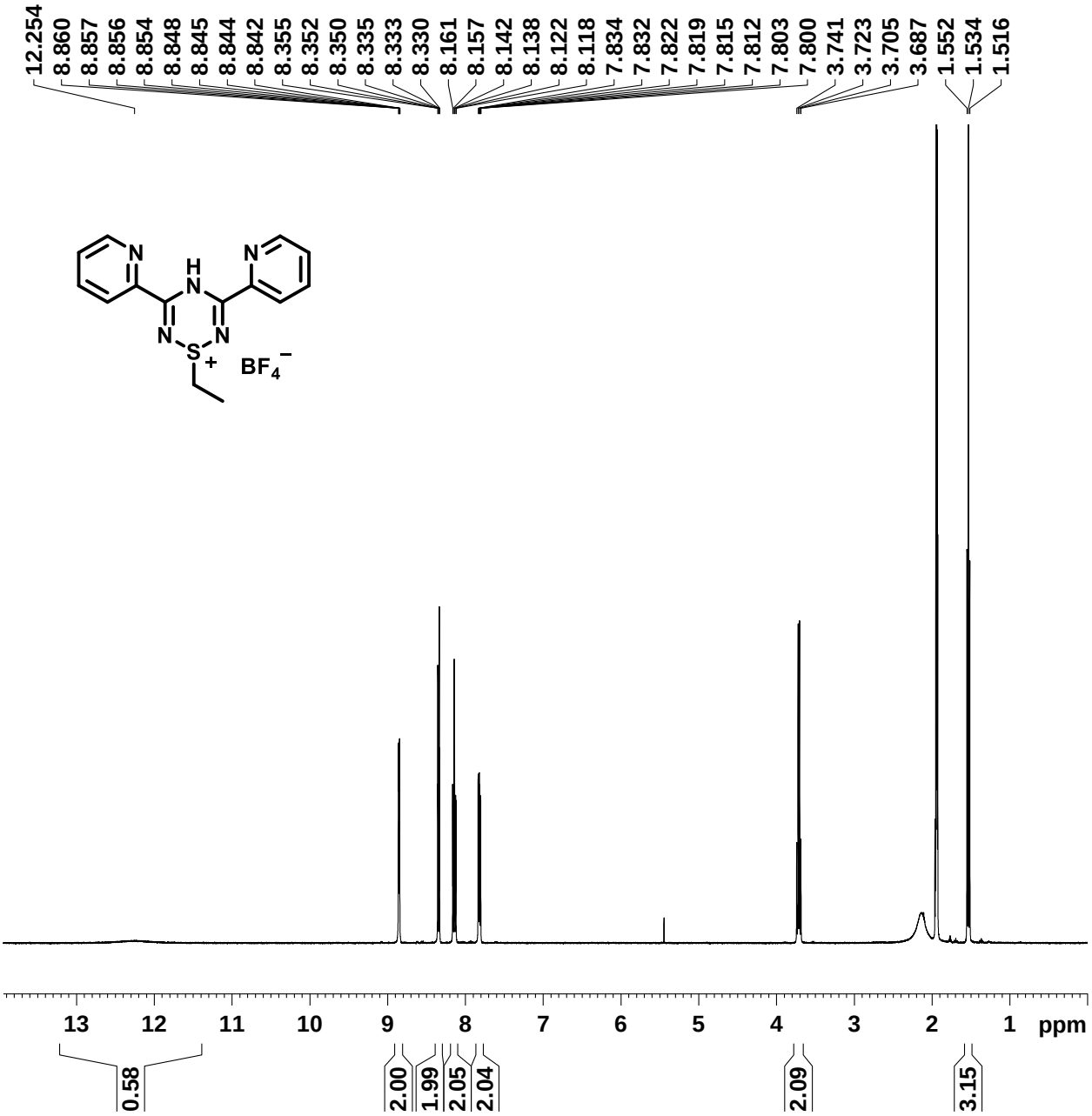

Figure S1. ^{1}H NMR spectrum of **12** in MeCN-d_3.

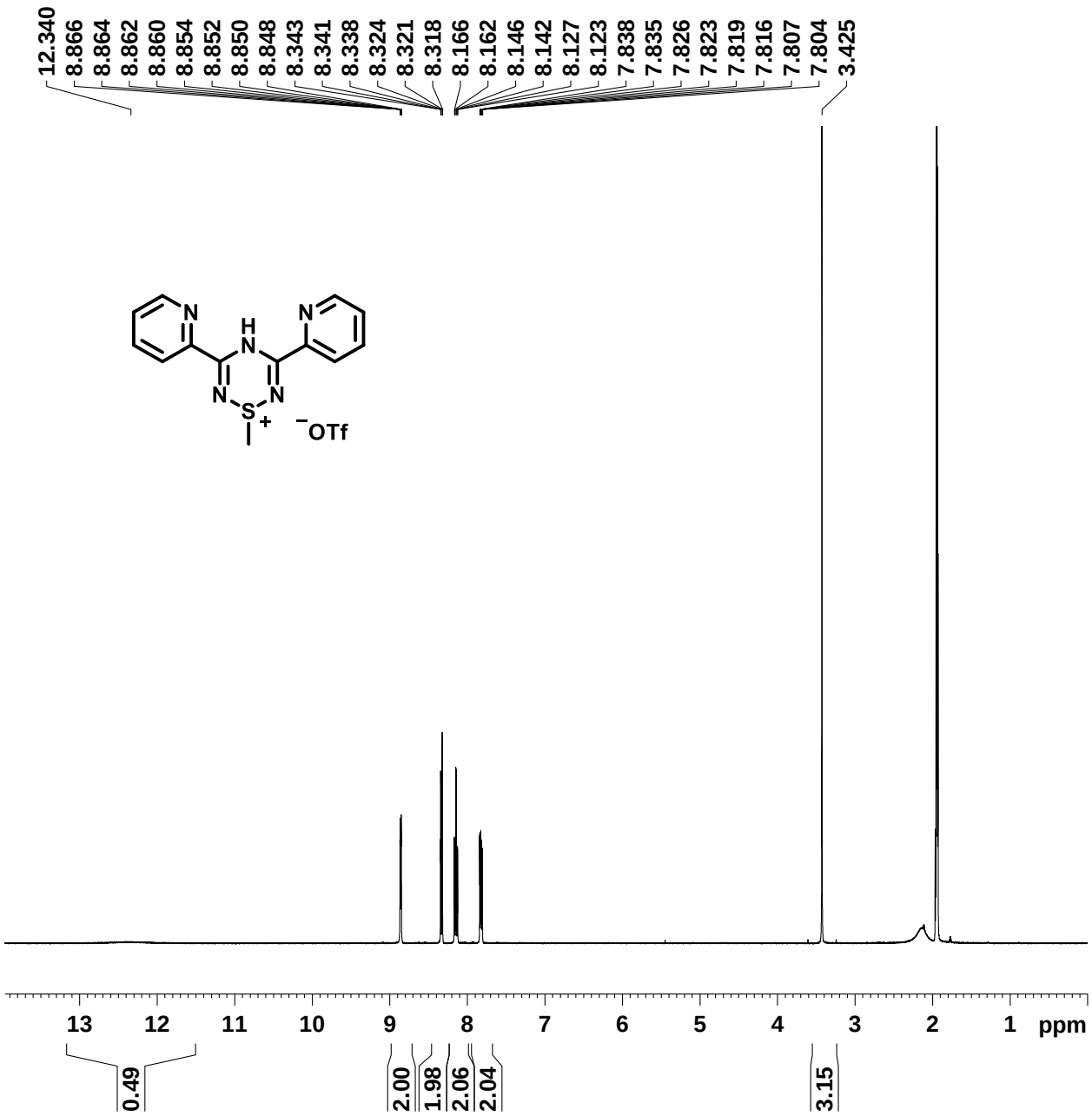

Figure S2. ^{1}H NMR spectrum of **13** in MeCN-d_3.

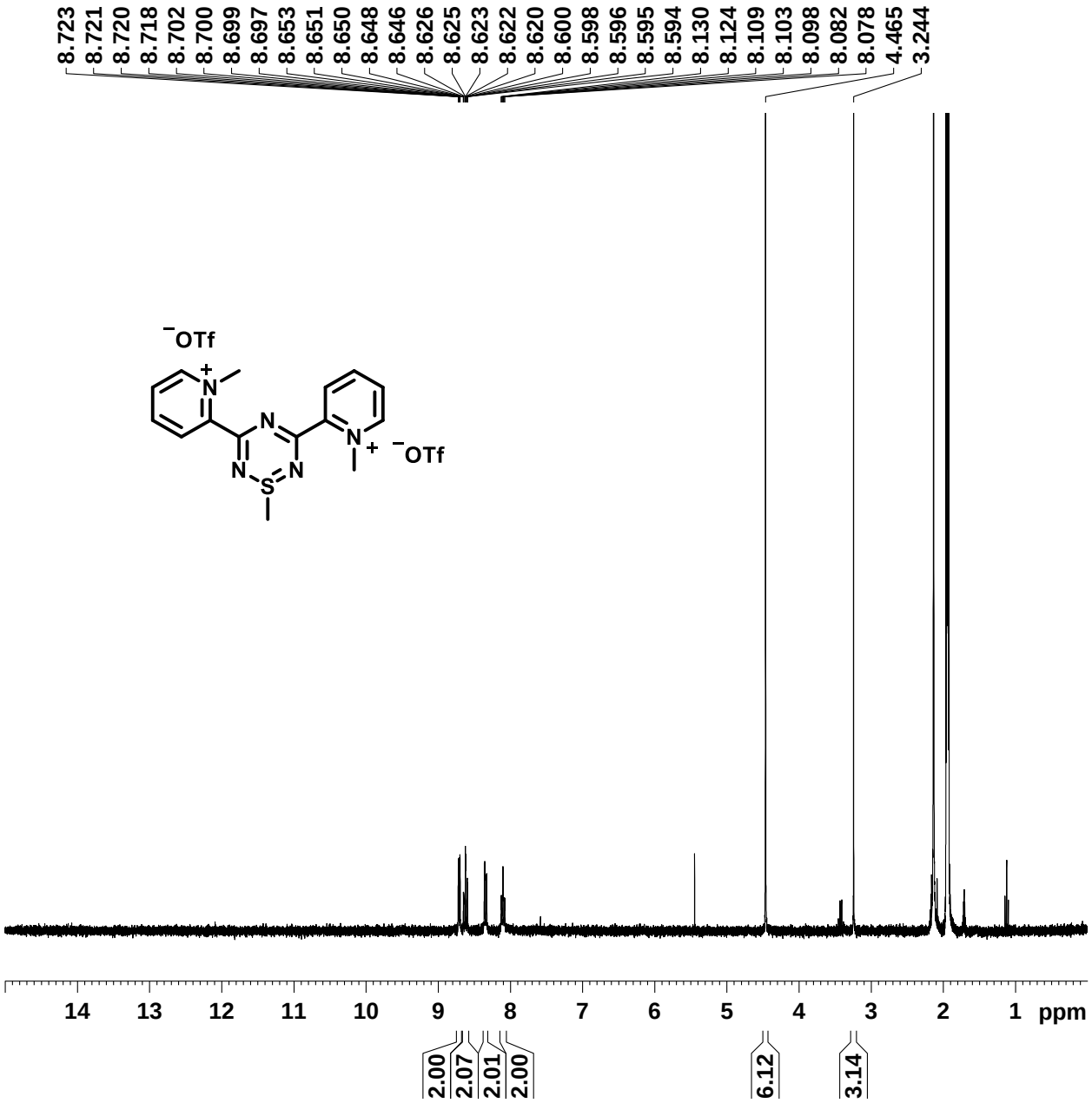

Figure S3. ^{1}H NMR spectrum of [**3,5-*bis*(*N*-methyl-2-pyridinium)-*S*-methyl-1,2,4,6-thiatriazine][OTf]$_2$** in MeCN-d$_3$.

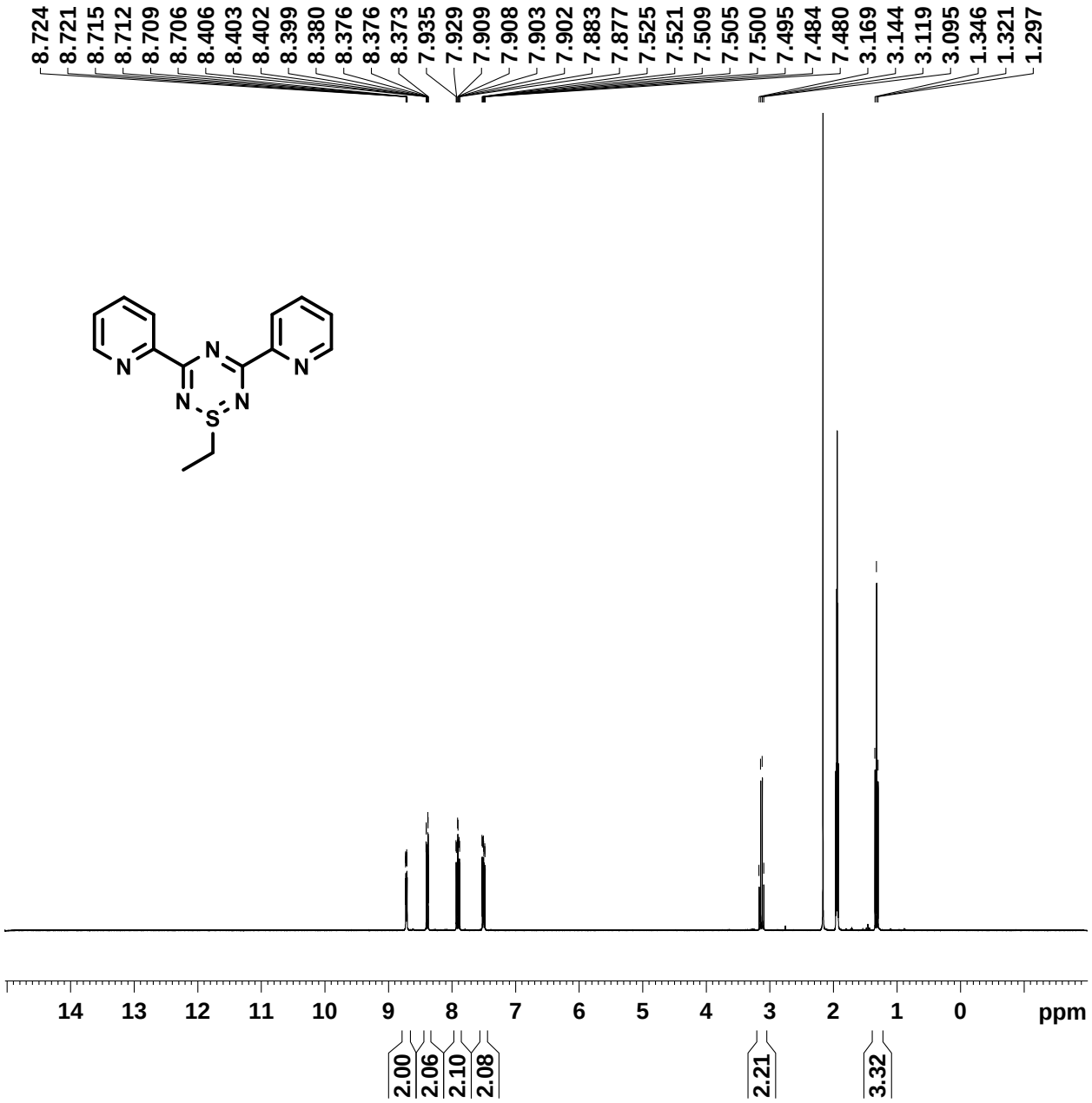

Figure S4. ^{1}H NMR spectrum of **14** in MeCN-d_3.

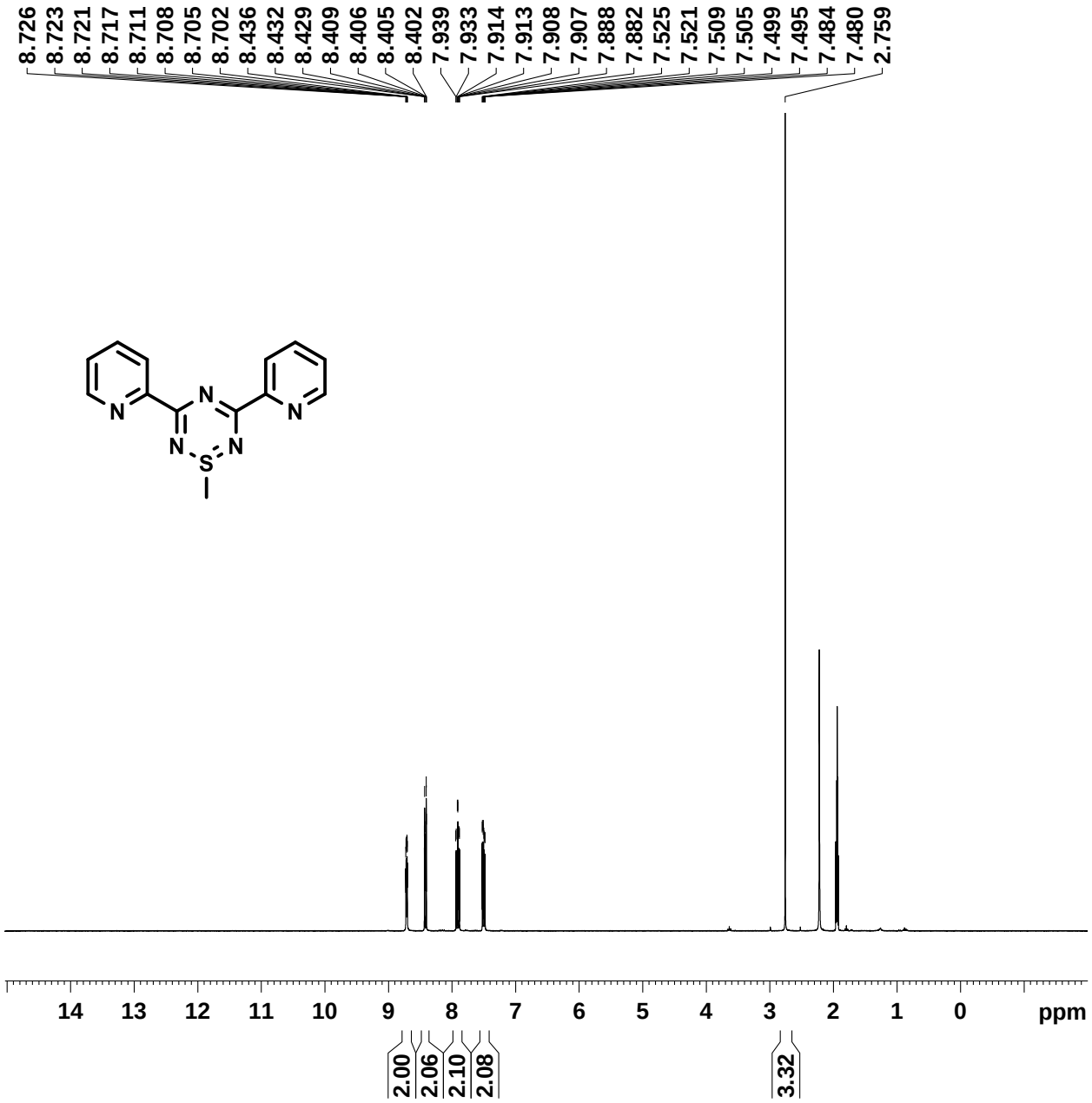

Figure S5. ^{1}H NMR spectrum of **15** in MeCN-d_3.

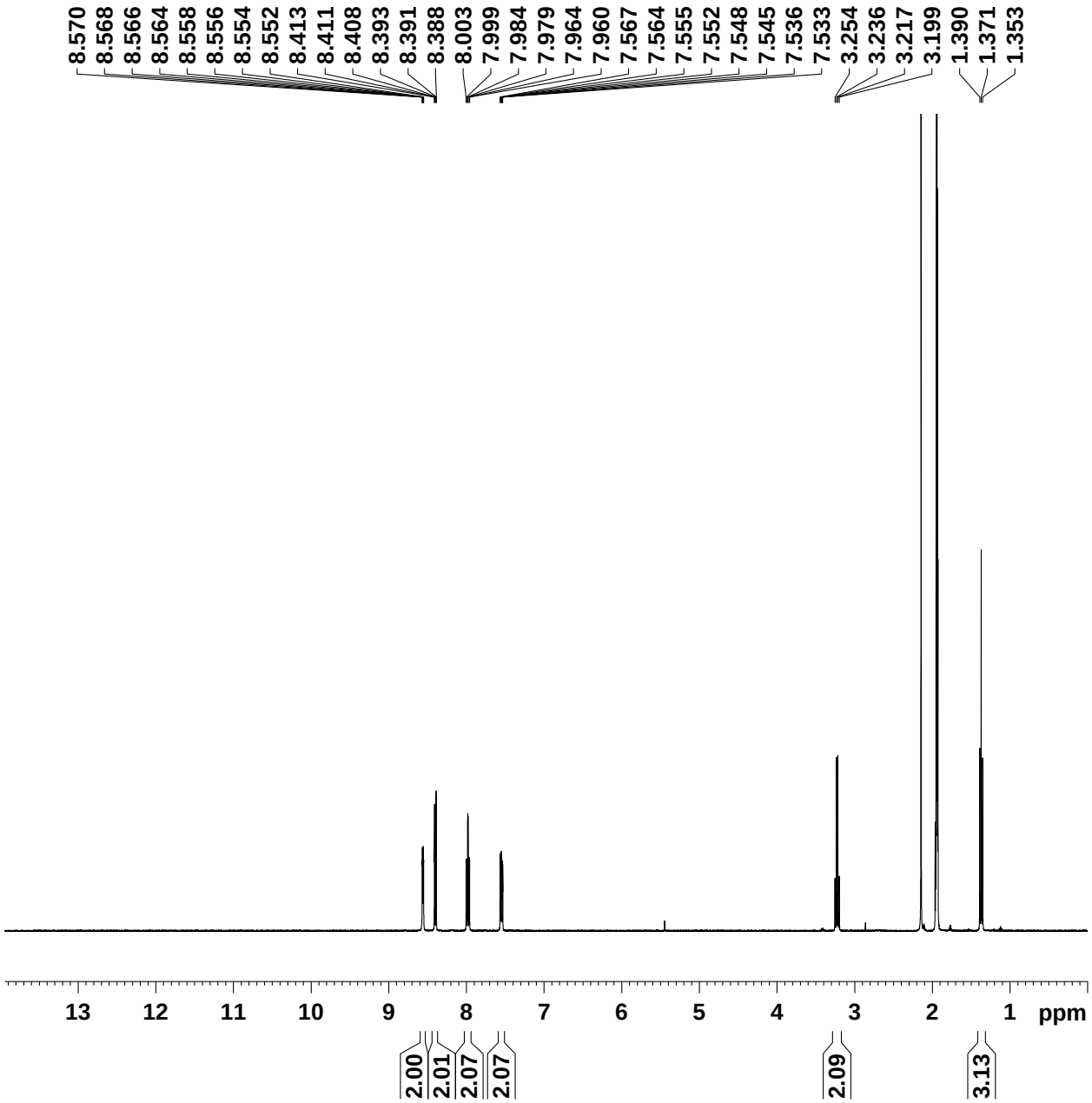

Figure S6. ^{1}H NMR spectrum of **17** in MeCN-d_3.

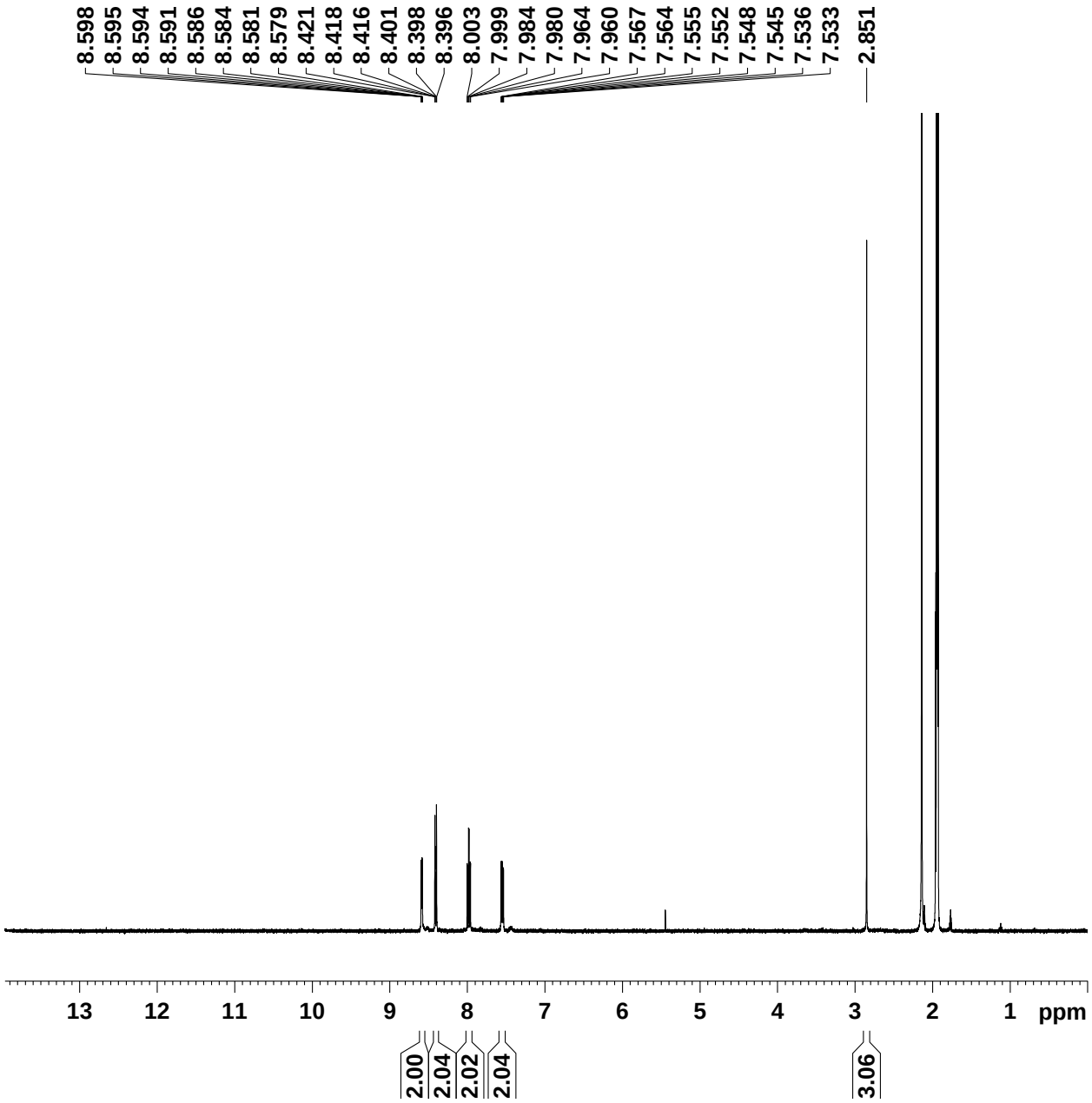

Figure S7. ^{1}H NMR spectrum of **18** in MeCN-d_3.

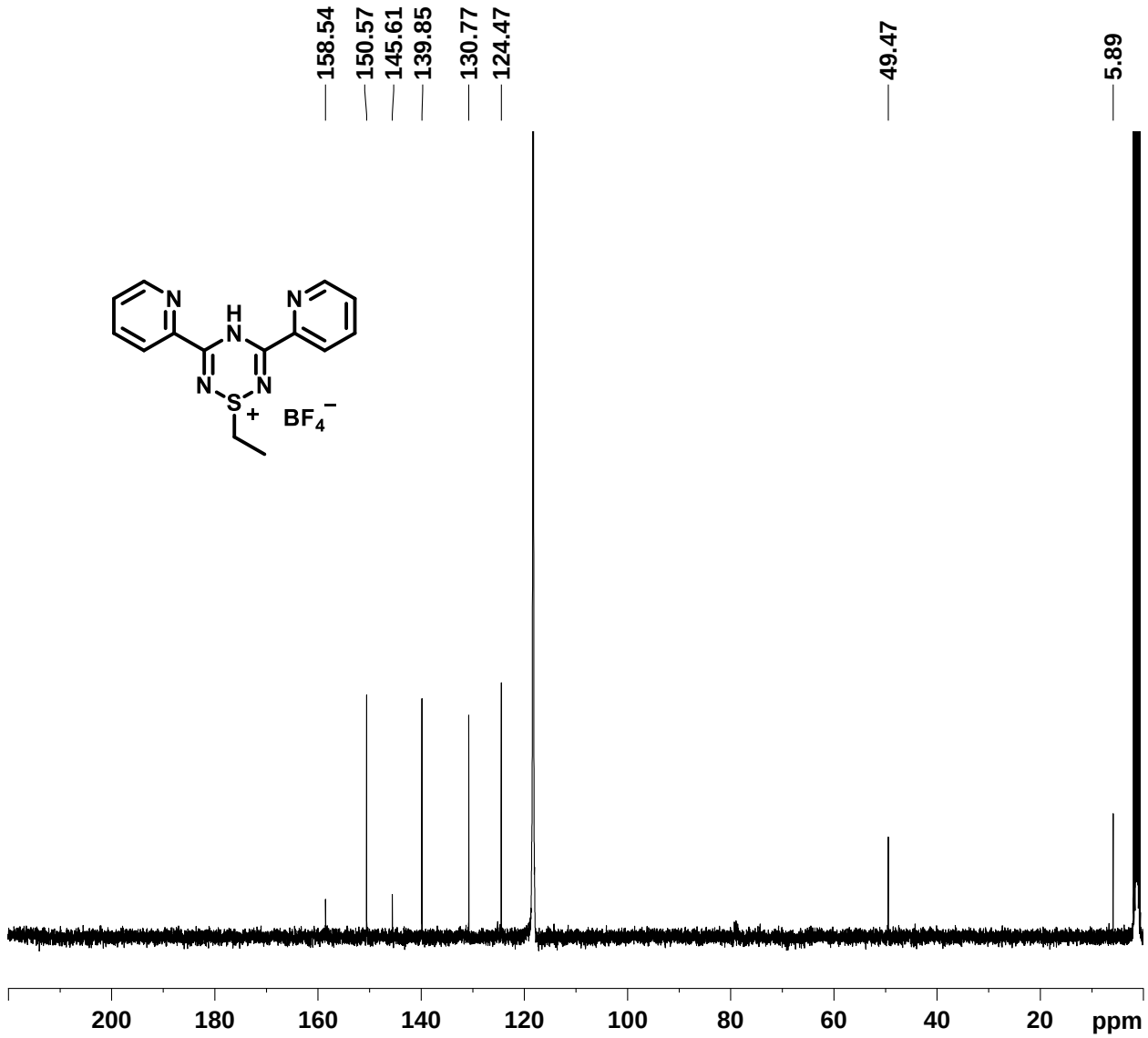

Figure S8. ^{13}C NMR spectrum of **12** in MeCN-d_3.

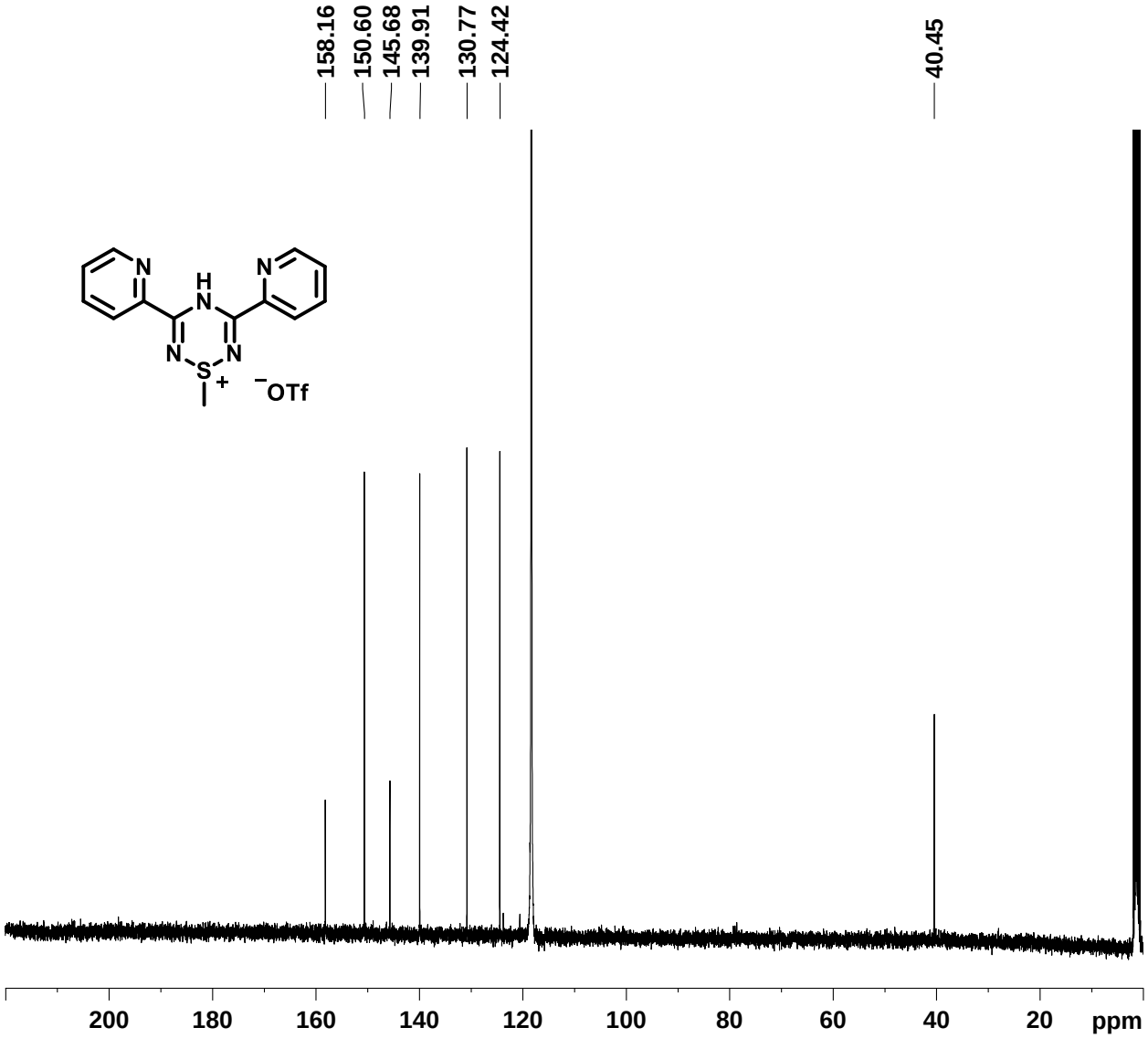

Figure S9. ^{13}C NMR spectrum of **13** in MeCN-d_3.

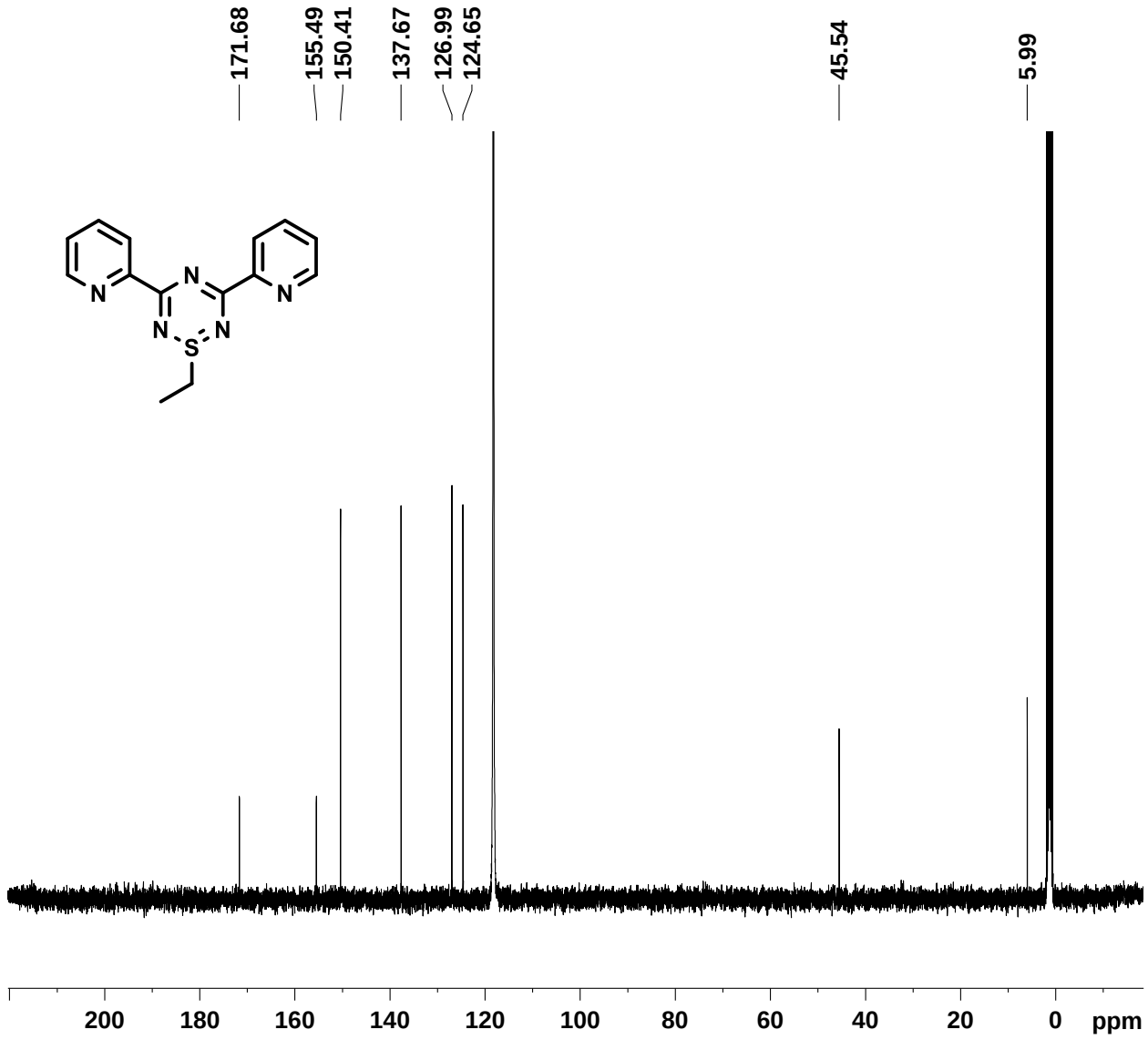

Figure S10. ^{13}C NMR spectrum of **14** in MeCN-d_3.

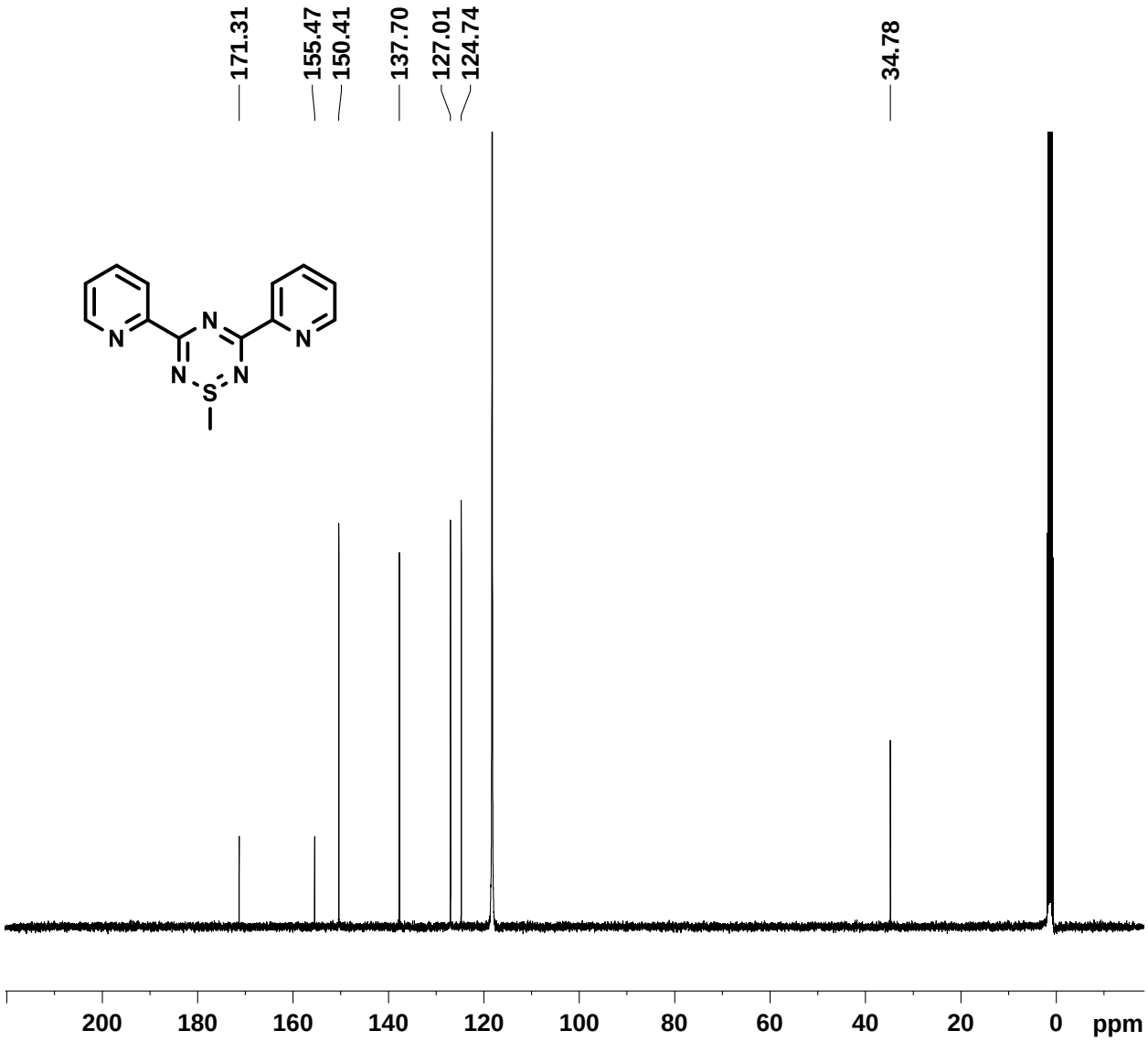

Figure S11. ^{13}C NMR spectrum of **15** in MeCN-d_3.

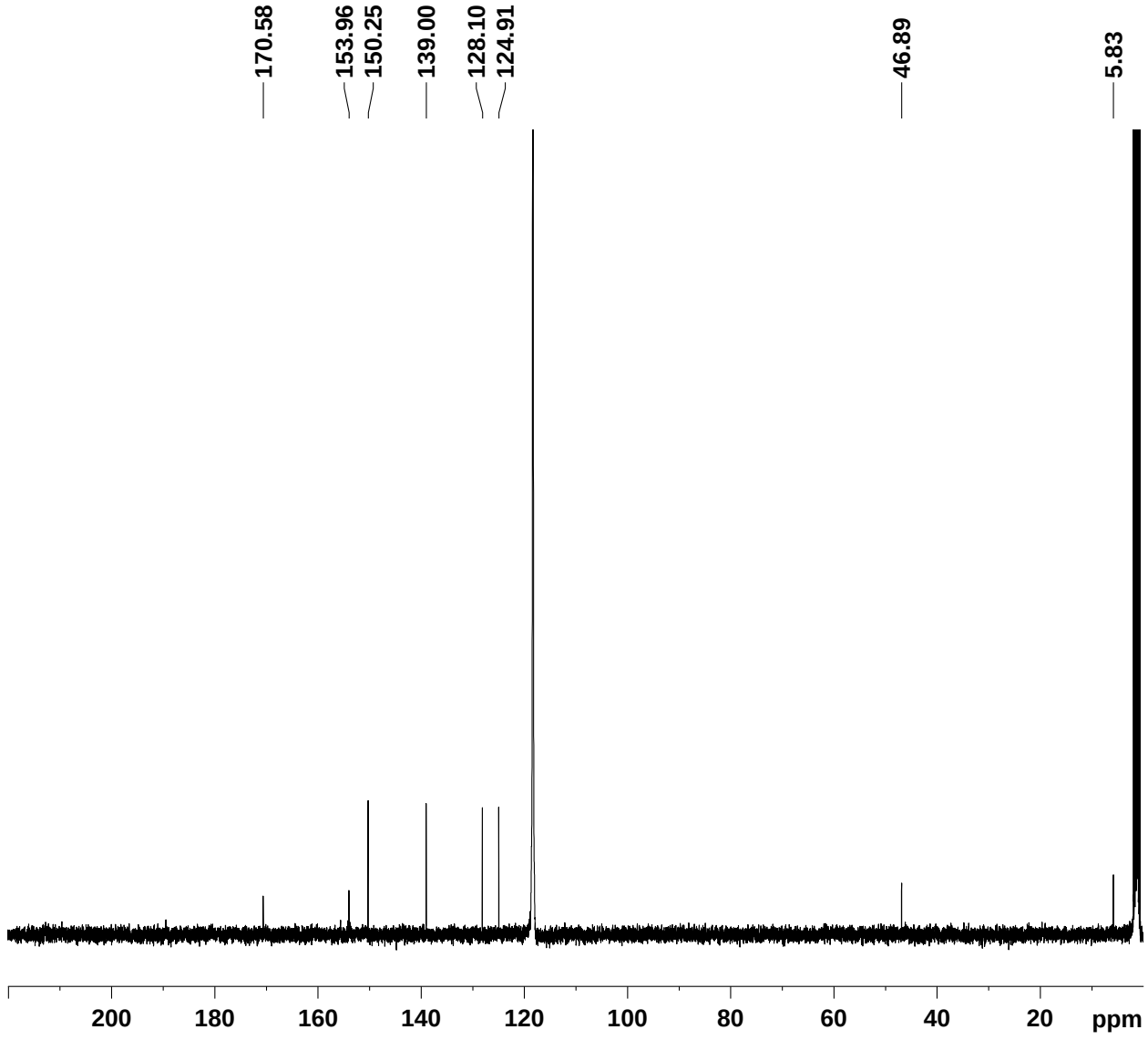

Figure S12. ^{13}C NMR spectrum of **17** in MeCN-d_3.

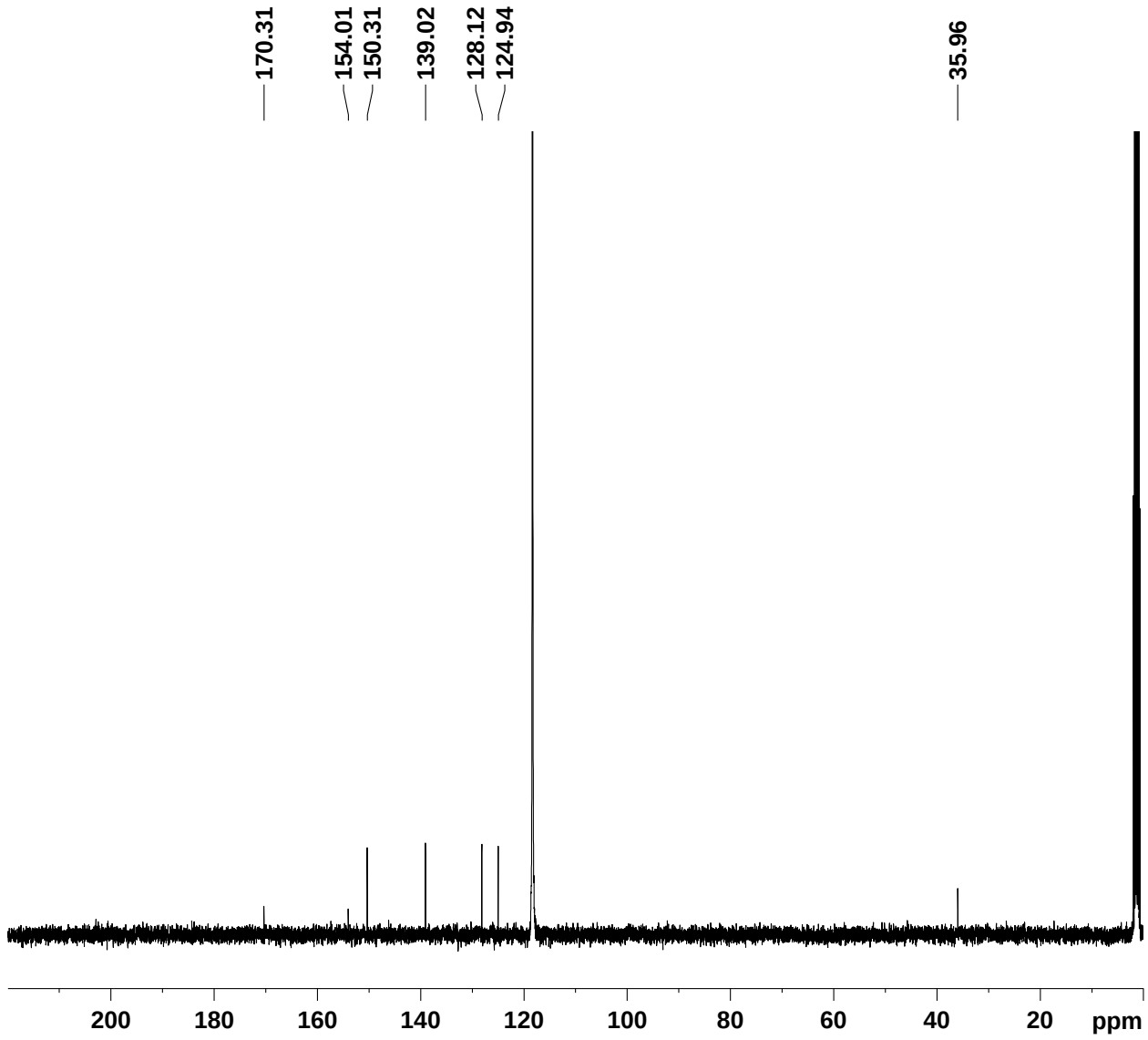

Figure S13. ^{13}C NMR spectrum of **18** in MeCN-d_3.

Table S1. Crystallographic data and selected collection parameters for **12**, **14**, [**3,5-*bis*(*N*-methyl-2-pyridinium)-*S*-methyl-1,2,4,6-thiatriazine][OTf]$_2$ ([(MePy)$_2$MeTTA][OTf]$_2$)** and **17**.

Parameters	**12**	**14**	**[(MePy)$_2$MeTTA][OTf]$_2$**	**17**
Empirical formula	$C_{14}H_{14}BF_4N_5S$	$C_{14}H_{13}N_5S$	$C_{17}H_{17}F_6N_5O_6S_3$	$C_{14}H_{13}IN_5NaS$
Formula weight	371.17	283.35	597.53	433.24
Crystal system	orthorhombic	orthorhombic	triclinic	triclinic
Space group	$P2_12_12_1$	$P2_12_12_1$	$P\bar{1}$	$P\bar{1}$
a (Å)	9.9995(2)	5.799(3)	8.938(4)	10.1629(3)
b (Å)	10.0313(2)	14.641(9)	11.927(5)	10.3262(3)
c (Å)	16.1233(4)	16.056(10)	12.900(5)	10.3488(3)
α (deg)	90	90	96.902(19)	109.4798(8)
β (deg)	90	90	108.004(18)	116.3682(8)
γ (deg)	90	90	107.987(17)	102.2525(9)
V (Å$_3$)	1617.30(6)	1363.2(14)	1208.1(8)	829.69(4)
Z	4	4	2	2
D_{calc} (mg/m3)	1.524	1.381	1.643	1.734
T (K)	200(2)	258(2)	200(2)	200(2)
μ (mm^{-1})	0.250	0.234	0.398	2.084
θ range for data collection (deg)	2.397 to 28.28	1.882 to 28.089	2.198 to 34.352	2.313 to 28.43
no. of total reflections	14055	11126	25311	8711
no. of unique reflections	3960	3294	9183	4062
R_{int}	0.0279	0.0331	0.0202	0.0109
R1, WR_2 (on F_2)	0.0424, 0.1191	0.0419, 0.0933	0.0485, 0.1266	0.0167, 0.0434

Table S2. Bond length comparisons of the central TTA ring for compounds **12**, **14**, [**3,5-*bis*(*N*-methyl-2-pyridinium)-*S*-methyl-1,2,4,6-thiatriazine][OTf]$_2$ ([(MePy)$_2$MeTTA][OTf]$_2$)** and **17**, as well as other previously reported TTA derivatives **[3,5-*bis*(*N*-hydro-2-pyrinium)-*S*-bromo-1,2,4,6-thiatriazine][Br][Br$_3$] ([(HPy)$_2$BrTTA][Br][Br$_3$])**,[1] **3,5-*bis*(pyridyl)-4-hydro-*S*-oxo-1,2,4,6-thiatriazine (Py$_2$TTAH=O)**[1] and **Py$_2$TTAH** (**11**).[2] Bond numbers are in reference to the numbers shown in the schematic, and all lengths are reported in Angstroms (Å).

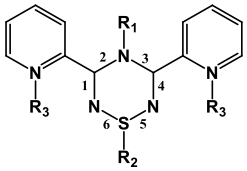	Aromatic				Anti-Aromatic		
	14 R_2=Et	**[(MePy)$_2$MeTTA][OTf]$_2$** R_2=Me, R_3=Me	**17** R_1=Na-I, R_2=Et	**[(HPy)$_2$BrTTA][Br][Br$_3$]** R_2=Br, R_3=Br	**12** R_1=H, R_2=Et	**11** R_1=H	**Py$_2$TTAH=O** R_1=H, R_2=O
1	1.3333(31)	1.3059(20)	1.3168(26)	1.3398(47)	1.2872(37)	1.279(2)	1.2854(43)
2	1.3394(32)	1.3571(17)	1.3409(17)	1.3378(52)	1.3556(31)	1.396(2)	1.3726(42)
3	1.3504(35)	1.3361(23)	1.3550(21)	1.3448(56)	1.3612(38)	1.391(2)	1.3671(42)
4	1.3157(31)	1.3195(22)	1.3117(26)	1.3181(48)	1.2858(37)	1.278(2)	1.2831(43)
5	1.6638(23)	1.6731(13)	1.6693(12)	1.6216(38)	1.6630(22)	1.693(2)	1.6865(27)
6	1.6544(23)	1.6705(18)	1.6521(19)	1.6027(42)	1.6728(25)	1.692(2)	1.6814(28)

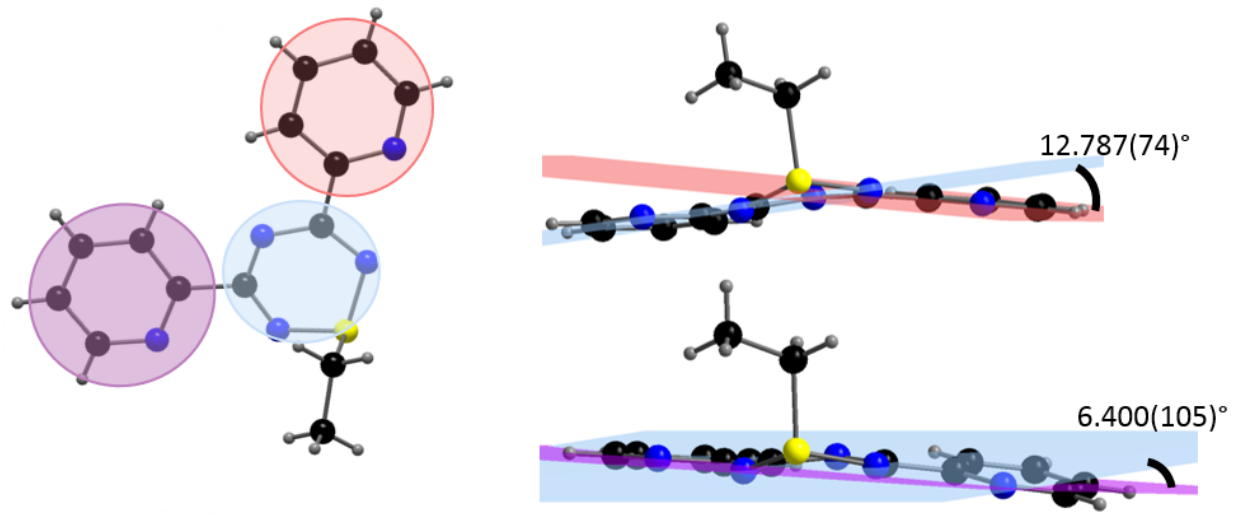

Figure S14. Calculated twist angles between planes of the thiatriazine and pyridine rings of **14**. The central plane was calculated without the S and N3 atoms, as this ring adopts a shallow boat-like arrangement.

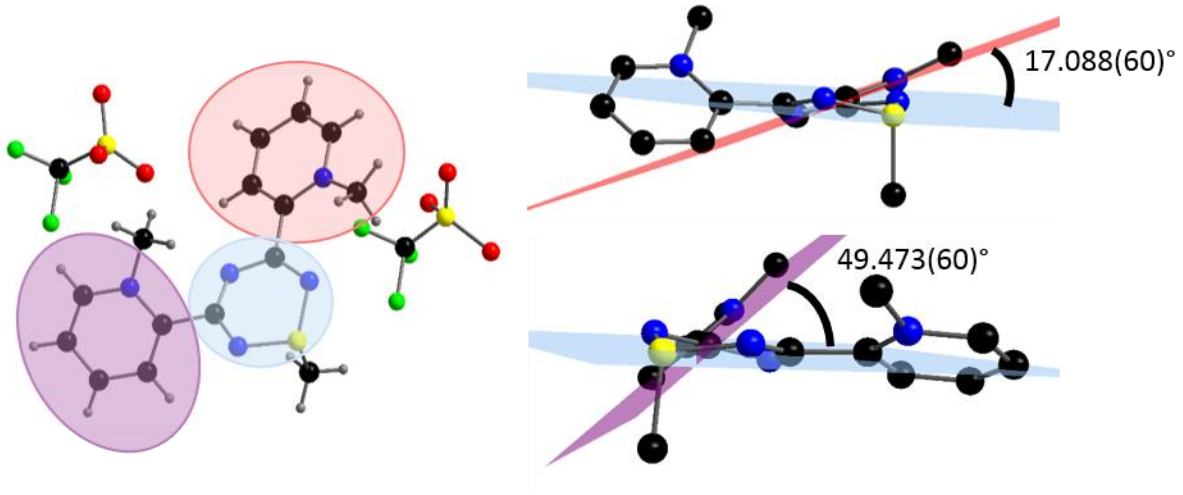

Figure S15. Calculated twist angles between planes of the thiatriazine and pyridine rings of [**3,5-*bis*(*N*-methyl-2-pyridinium)-*S*-methyl-1,2,4,6-thiatriazine][OTf]**$_2$. The central plane was calculated without the S11 and N22 atoms, as this ring adopts a shallow boat-like arrangement. Hydrogens removed for clarity (left).

Table S3: Frontier molecular orbitals and corresponding energies (in eV) for **14**, **15**, and **11**. Energies were calculated at the B3LYP/6-311+G(2d,p) level of theory, and orbital probability diagrams were generated using GaussView 5.0 software.[3]

	14	**15**	**11**
LUMO+2	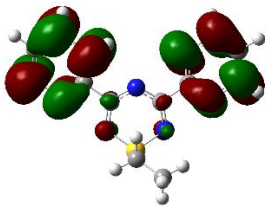 -0.977226	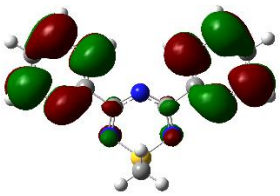 -1.12846	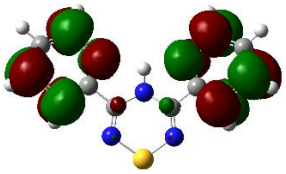 -1.24710
LUMO+1	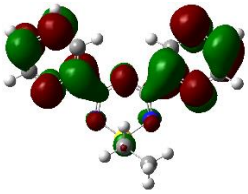 -1.28628	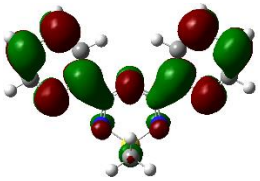 -1.49472	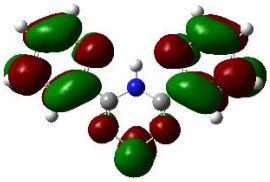 -1.57227
LUMO	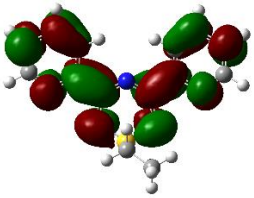 -2.27324	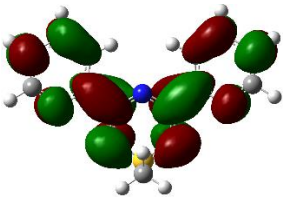 -2.53801	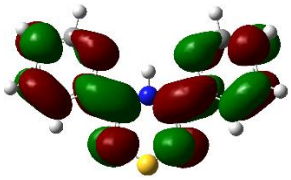 -2.26861
HOMO	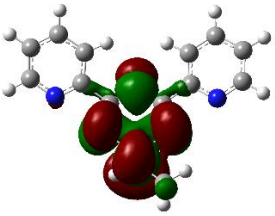 -6.22216	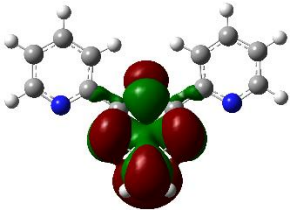 -6.60013	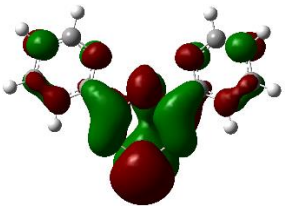 -5.28364
HOMO-1	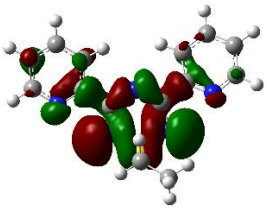 -7.01592	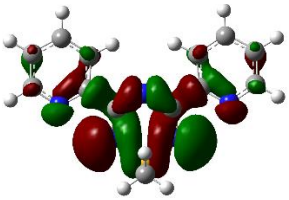 -7.30626	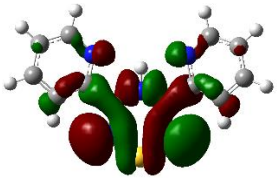 -7.40014
HOMO-2	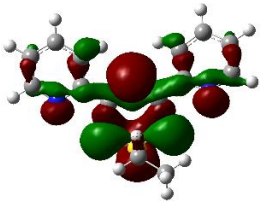 -7.09891	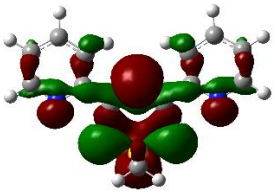 -7.38463	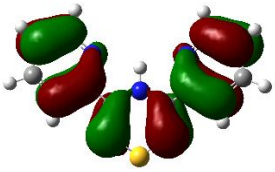 -7.54545

Table S4 – TD DFT optical transitions[a] for **14** and **15**, calculated at the B3LYP/6-311+G(2d,p) level of theory on geometry optimized structures with Gaussian 09 software.[3]

k	**14**		**15**	
	E (eV)	*f*	E (eV)	*f*
1	3.1469	0.0276	3.2206	0.0273
2	3.8194	0.0250	3.7961	0.0408
3	3.9578	0.0071	3.9157	0.0046
4	4.2397	0.0429	4.2561	0.1391
5	4.2852	0.0829	4.2670	0.0293
6	4.3775	0.2499	4.4441	0.0153
7	4.3898	0.0703	4.4444	0.2303
8	4.5744	0.1362	4.5399	0.1592
9	4.7329	0.0581	4.8148	0.0405
10	4.7701	0.0093	4.8729	0.0097
11	5.0354	0.0025	5.0133	0.0012
12	5.0839	0.0041	5.0669	0.0013
13	5.0906	0.0043	5.0793	0.0003
14	5.1081	0.0093	5.0827	0.084
15	5.1274	0.0200	5.0834	0.0002
16	5.1886	0.0501	5.1349	0.0686
17	5.3649	0.1191	5.3638	0.1637
18	5.3779	0.1082	5.4066	0.0727
19	5.4587	0.0232	5.5428	0.0277
20	5.5231	0.0153	5.5823	0.0111

[a] k = order of excitation energy and *f* = oscillator strength.

Table S5 – Selected TD DFT transitions for **14**. Transitions shown are those with the greatest calculated oscillator strength, as well as the HOMO to LUMO transition. Calculations were performed at the B3LYP/6-311+G(2d,p) level of theory with acetonitrile solvation using Gaussian 09 software.[3]

Calculated λ (nm)	Transitions	Oscillator Strength (*f*)
394	HOMO → LUMO	0.0276
283	HOMO-6 → LUMO HOMO-5 → LUMO HOMO-4 → LUMO HOMO-3 → LUMO HOMO-2 →LUMO HOMO-1 → LUMO HOMO → LUMO+1	0.2499
271	HOMO-6 → LUMO HOMO-5 → LUMO HOMO-4 → LUMO HOMO-3 → LUMO HOMO-2 → LUMO HOMO-1 → LUMO HOMO → LUMO+2	0.1362
231	HOMO-8 → LUMO HOMO-5 → LUMO+1 HOMO-4 → LUMO+1 HOMO-2 → LUMO+1 HOMO → LUMO+4	0.1191
230	HOMO-8 → LUMO HOMO-5 → LUMO+1 HOMO-4 → LUMO+1 HOMO-2 → LUMO+1 HOMO → LUMO+4	0.1082

Table S6 – Selected TD DFT transitions for **15**. Transitions shown are those with the greatest calculated oscillator strength, as well as the HOMO to LUMO transition. Calculations were performed at the B3LYP/6-311+G(2d,p) level of theory with acetonitrile solvation using Gaussian 09 software.[3]

Calculated λ (nm)	Transitions	Oscillator Strength (*f*)
385	HOMO → LUMO	0.0273
291	HOMO-6 → LUMO HOMO-4 → LUMO+1 HOMO-3 → LUMO HOMO-2 → LUMO+1	0.1391
279	HOMO-5 → LUMO HOMO-3 → LUMO HOMO-1 → LUMO	0.2303
273	HOMO-5 → LUMO HOMO-4 → LUMO HOMO-2 → LUMO HOMO → LUMO+2	0.1592
231	HOMO-8 → LUMO HOMO-5 → LUMO+1 HOMO-4 → LUMO+1 HOMO-2 → LUMO+1	0.1637

Table S7 – Comparative table for the measured molar coefficients of extinction[a] with the corresponding calculated oscillator strengths[b] for **14** and **15**.

	λ (nm)	ε ($\mu M^{-1}cm^{-1}$)	Calculated λ (nm)	*f*
14	240	0.0161	230	0.1082
			231	0.1191
	275	0.0196	271	0.1362
			283	0.2499
	390	0.0018	394	0.0276
15	240	0.0164	231	0.1637
	275	0.0195	273	0.1592
			279	0.2303
			291	0.1391
	390	0.0019	385	0.0273

[a] Optical measurements were performed on dilute MeCN solutions. [b] TD DFT/B3LYP/6-311+G(2d,p) level of theory on geometry optimized structures where *f* = oscillator strength using Gaussian 09 software.[3]

References

1. A. A. Leitch, I. Korobkov, A. Assoud and J. L. Brusso, *Chemical Communications*, 2014, **50**, 4934-4936.
2. N. J. Yutronkie, A. A. Leitch, I. Korobkov and J. L. Brusso, *Crystal Growth & Design*, 2015, **15**, 2524-2532.
3. M. J. Frisch, G. W. Trucks, H. B. Schlegel, G. E. Scuseria, M. A. Robb, J. R. Cheeseman, G. Scalmani, V. Barone, B. Mennucci, G. A. Petersson, H. Nakatsuji, M. Caricato, X. Li, H. P. Hratchian, A. F. Izmaylov, J. Bloino, G. Zheng, J. L. Sonnenberg, M. Hada, M. Ehara, K. Toyota, R. Fukuda, J. Hasegawa, M. Ishida, T. Nakajima, Y. Honda, O. Kitao, H. Nakai, T. Vreven, J. J. A. Montgomery, J. E. Peralta, F. Ogliaro, M. Bearpark, J. J. Heyd, E. Brothers, K. N. Kudin, V. N. Staroverov, R. Kobayashi, J. Normand, K. Raghavachari, A. Rendell, J. C. Burant, S. S. Iyengar, J. Tomasi, M. Cossi, N. Rega, J. M. Millam, M. Klene, J. E. Knox, J. B. Cross, V. Bakken, C. Adamo, J. Jaramillo, R. Gomperts, R. E. Stratmann, O. Yazyev, A. J. Austin, R. Cammi, C. Pomelli, J. W. Ochterski, R. L. Martin, K. Morokuma, V. G. Zakrzewski, G. A. Voth, P. Salvador, J. J. Dannenberg, S. Dapprich, A. D. Daniels, O. Farkas, J. B. Foresman, J. V. Ortiz, J. Cioslowski and D. J. Fox, *Gaussian 09*, Revision A.02; Gaussian, Inc.: Wallingford, CT, 2009.